Electronic Supporting Information

High-yield synthesis and catalytic response of chainlike hybrid materials of the [$(MoO_3)_m$(2,2'-bipyridine)$_n$] family

Sofia M. Bruno, Lucie S. Nogueira, Ana C. Gomes, Anabela A. Valente, Isabel S. Gonçalves and Martyn Pillinger*

Department of Chemistry, CICECO - Aveiro Institute of Materials, University of Aveiro, Campus Universitário de Santiago, 3810-193 Aveiro, Portugal
E-mail: mpillinger@ua.pt (M. Pillinger)

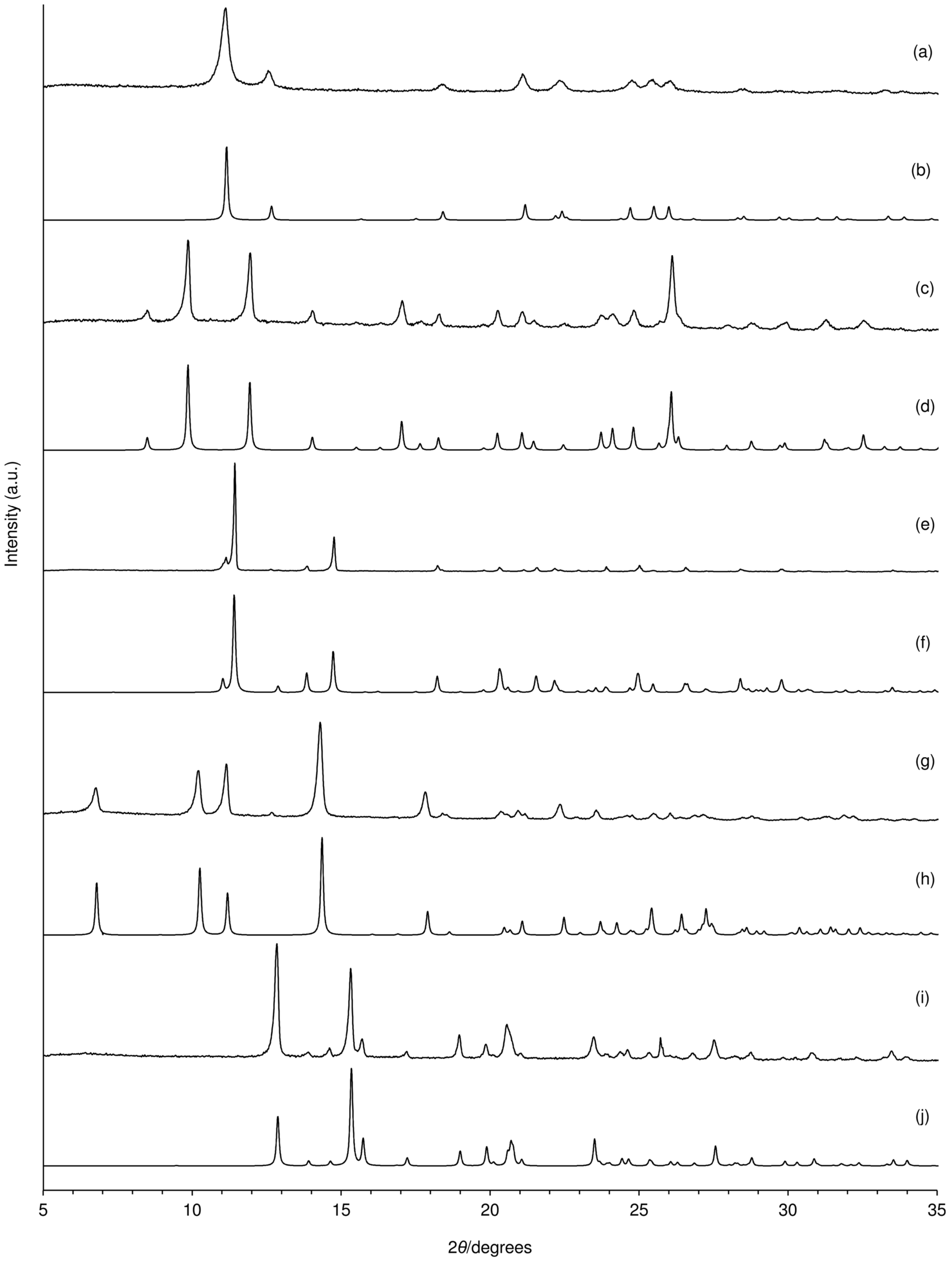

Fig. S1 Experimental (a,c,e,g,i) and computed (b,d,f,h,j) PXRD patterns of (a,b) **1**, (c,d) **2**, (e,f) **3**, (g,h) **4**, (i,j) **5**. The program Mercury (copyright CCDC, ver. 3.9)[1] was used to generate the computed patterns from the crystal structure data published for **1**-**3**,[2] **4**,[3] and **5**.[4]

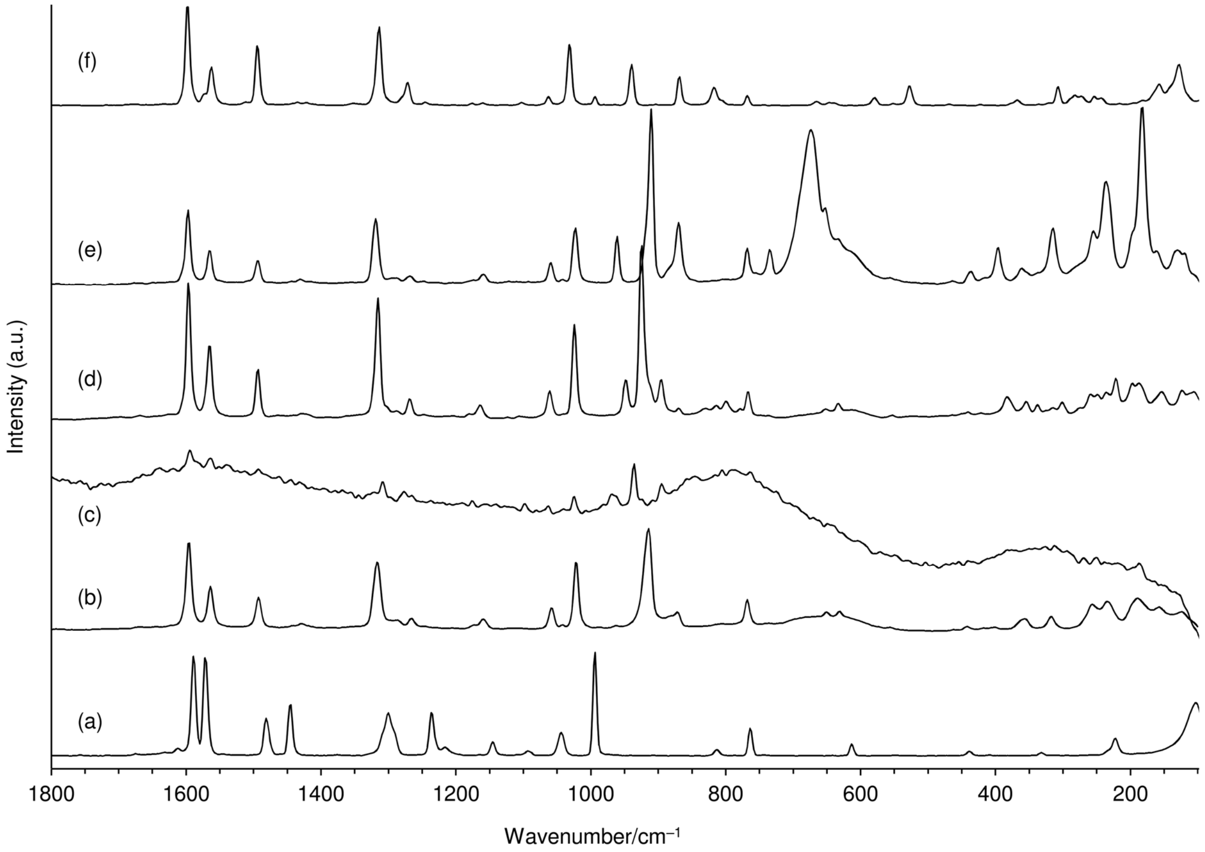

Fig. S2 FT-Raman spectra in the range of 100-1800 cm^{-1} for (a) 2,2'-bipy, (b) **1**, (c) **2**, (d) **3**, (e) **4** and (f) **5**.

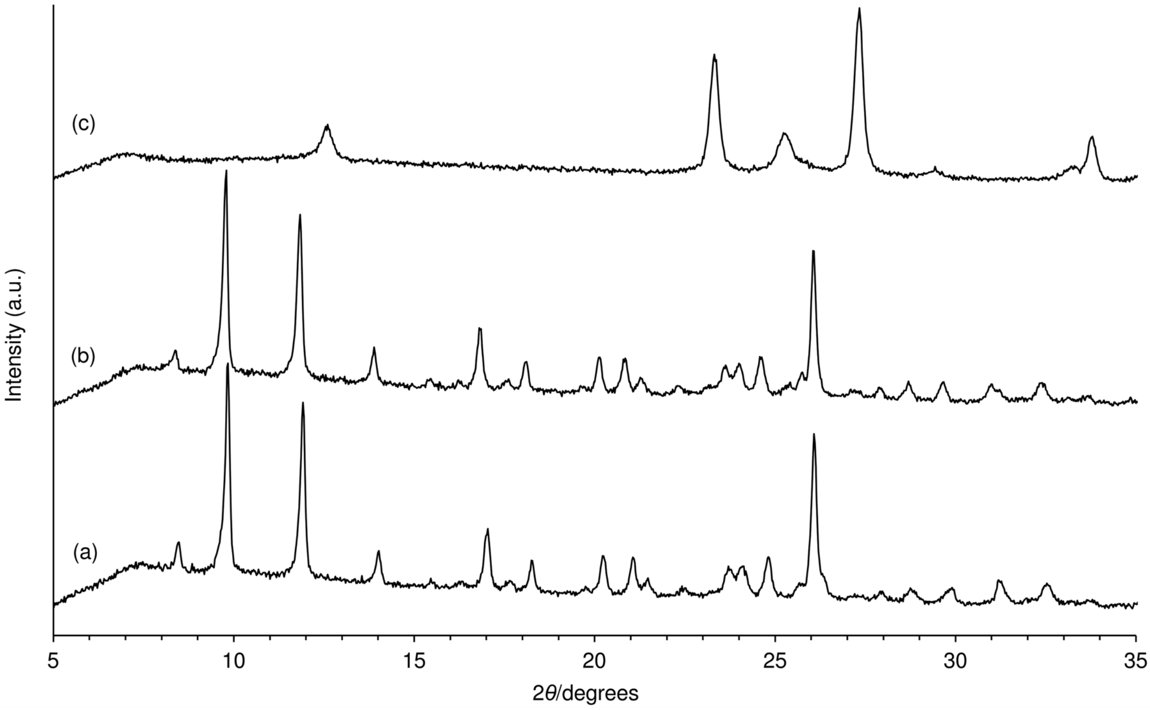

Fig. S3 Variable temperature PXRD study of [Mo_2O_6(2,2'-bipy)] (**2**): (a) ambient temperature, (b) 285 °C and (c) 420 °C.

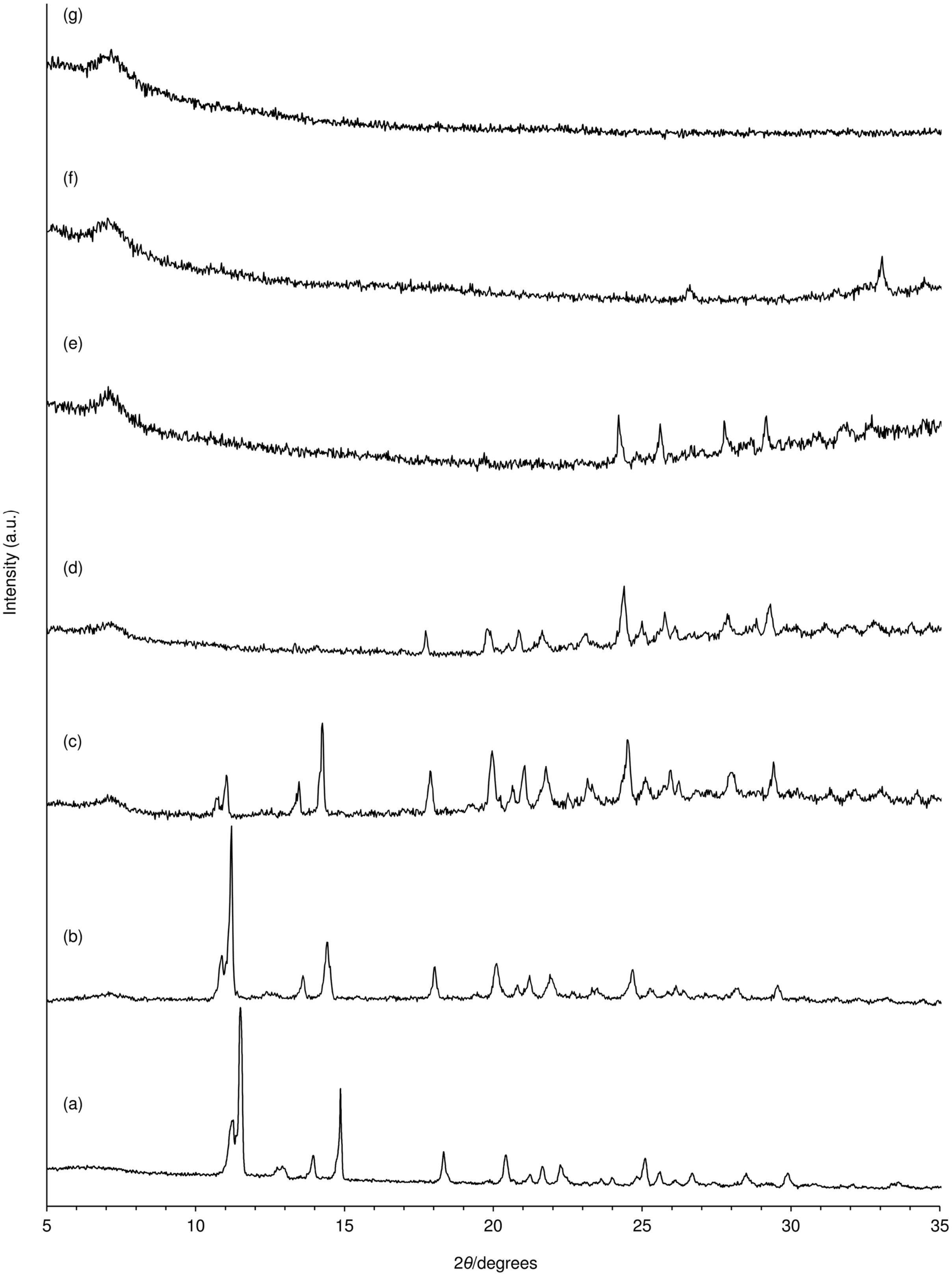

Fig. S4 Variable temperature PXRD study of $[Mo_3O_9(2,2'\text{-bipy})_2]$ (**3**): (a) ambient temperature, (b) 250 °C, (c) 280 °C, (d) 315 °C, (e) 360 °C, (f) 450 °C and (g) 700 °C.

Lewis acid activity of the molybdenum compounds

The Lewis acidity of compounds **1**-**4** was assessed through the model acid reaction of styrene oxide (StyO) with ethanol at 55 °C (the same temperature as that used for catalytic epoxidation, and without oxidant). Based on the literature, the reaction mechanism of the Lewis acid-catalysed reaction of the epoxide in alcohol media may involve the interaction of the Mo centre and the oxygen atom of epoxide, followed by nucleophilic attack of the alcohol reagent at the more substituted carbon atom of the oxirane, leading to the formation of the corresponding β-alkoxy alcohol product.[5,6]

The catalytic tests with StyO (Fluka, >97 %) and absolute ethanol (Carlos Erba) were carried out in a similar fashion to that described in the main article for catalytic epoxidation. For all molybdenum compounds tested, 2-ethoxy-2-phenylethanol (EPE) was always the only reaction product with 70-100 % yield at 24 h reaction (Table S1). Compounds **1**-**4** led to superior catalytic results than **5** and MoO_3; catalysts **2** and **4** led to the highest EPE yields (Table S1). The reaction without catalyst gave 6 % conversion at 24 h.

The solid phases recovered from the biphasic solid-liquid reaction mixtures after 24 h batch runs (denoted ***i***-AcidCat, ***i*** = **1**-**4**) were characterised by ATR FT-IR spectroscopy (Fig. S5) and powder XRD (Fig. S6), which indicated that the structural features were preserved and the compounds were stable.

Contact tests (CTs) were carried out for **1**-**4** in a similar fashion to that described in the main article for the catalysts tested in the epoxidation reaction systems. Specifically, the catalyst and solvent (without substrate) were stirred for 24 h at 55 °C, after which the solid (***i***-CT-Acid-S, ***i*** = **1**-**4**) and liquid (***i***-CT-Acid-L) phases were separated by centrifugation and membrane filtration. The liquid and solid phases obtained from the CTs were tested separately for StyO reaction at 55 °C. The reaction of StyO using ***i***-CT-Acid-L led to significant conversion, indicating that the catalytic reactions occurred in homogeneous phase; StyO conversion at 24 h of StyO reaction was 74, 100, 69 and 83 % for **1**, **2**, **3**, and **4**, respectively (Fig. S7). The solids ***i***-CT-Acid-S recovered from the CTs exhibited similar ATR FT-IR spectra (Fig. S5) and powder XRD patterns (Fig. S6) to those for the respective original catalysts, and no drop in conversion at 24 h was verified in relation to the respective original catalysts (Fig. S7). Moreover, the catalysts (***i***-CT-Acid-S-Cat) which were recovered from a 24 h batch run of StyO reaction in the presence of ***i***-CT-Acid-S exhibited similar ATR FT-IR spectra (Fig. S5) to the respective original catalysts. These results further confirm the fairly good stability of the studied catalysts, under the alcoholysis reaction conditions.

Table S1 Acid-catalysed reaction of StyO with ethanol in the presence of **1**-**5** and MoO_3.[a]

Catalyst	StyO conversion at 6 h / 24 h (%)
$[MoO_3(2,2'\text{-bipy})]$ (**1**)	86/99
$[Mo_2O_6(2,2'\text{-bipy})]$ (**2**)	91/100
$[Mo_3O_9(2,2'\text{-bipy})_2]$ (**3**)	36/70
$\{[MoO_3(2,2'\text{-bipy})][MoO_3(H_2O)]\}_n$ (**4**)	97/100
$[MoO(O_2)_2(2,2'\text{-bipy})]$ (**5**)	64/66
MoO_3	42/99

[a] Reaction conditions: Mo:StyO = 1:10, 55 °C, 0.38 M StyO in ethanol (2 mL).

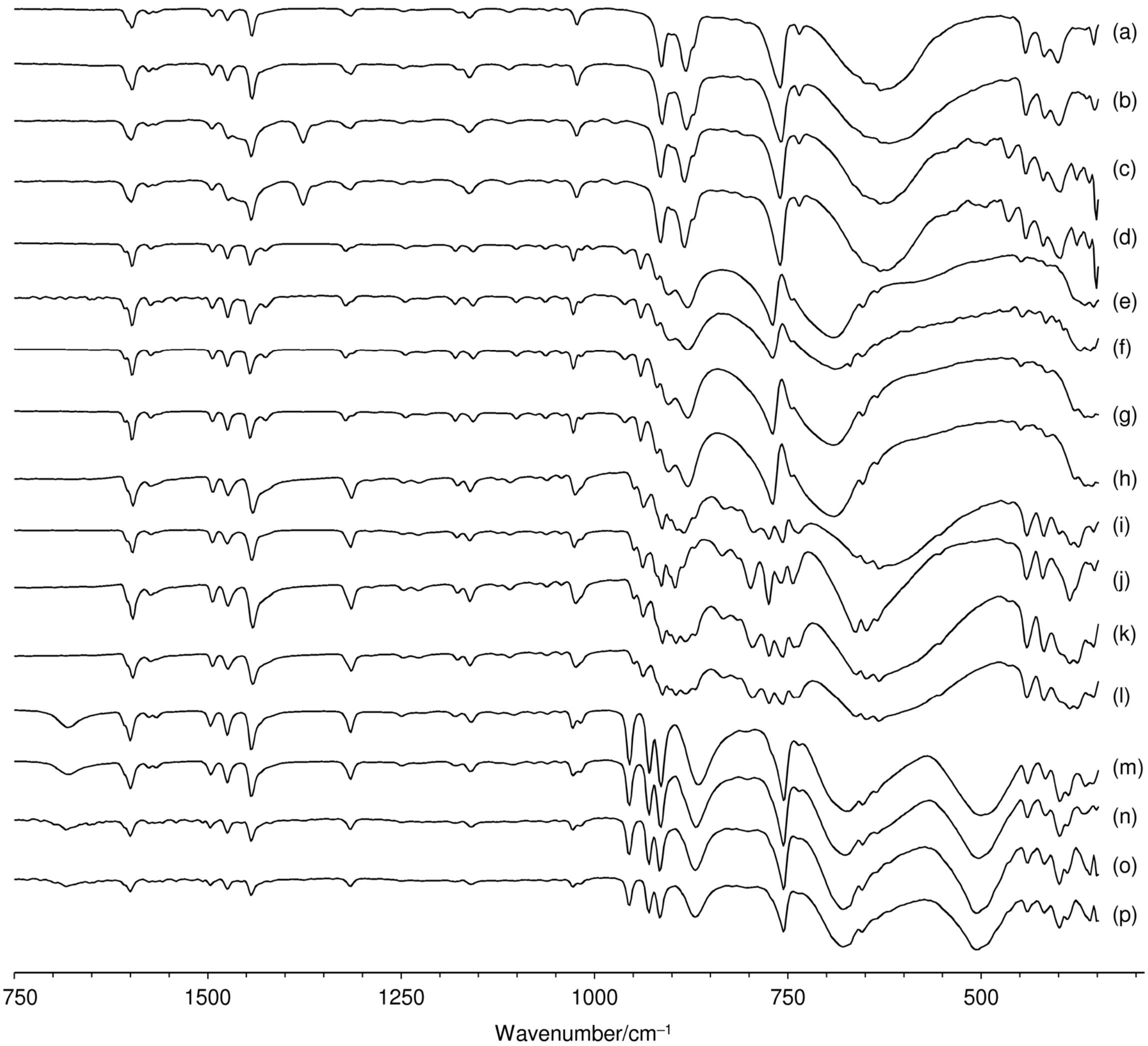

Fig. S5 ATR FT-IR spectra of (a) **1**, (b) **1**-AcidCat, (c) **1**-CT-Acid-S**,** (d) **1**-CT-Acid-S-Cat, (e) **2**, (f) **2**-AcidCat, (g) **2**-CT-Acid-S**,** (h) **2**-CT-Acid-S-Cat, (i) **3**, (j) **3**-AcidCat, (k) **3**-CT-Acid-S**,** (l) **3**-CT-Acid-S-Cat, (m) **4**, (n) **4**-AcidCat, (o) **4**-CT-Acid-S**,** and (p) **4**-CT-Acid-S-Cat.

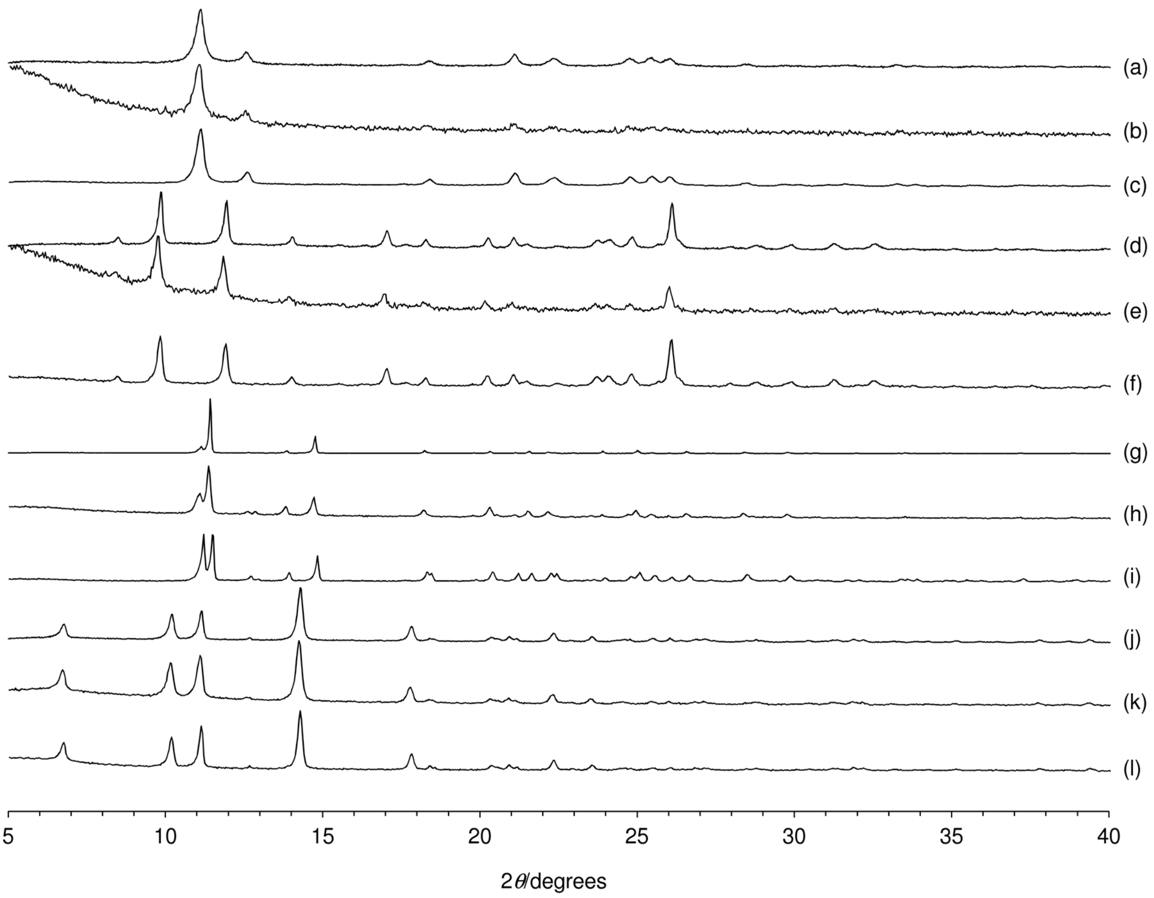

Fig. S6 PXRD patterns of (a) **1**, (b) **1**-AcidCat, (c) **1**-CT-Acid-S, (d) **2**, (e) **2**-AcidCat, (f) **2**-CT-Acid-S**,** (g) **3**, (h) **3**-AcidCat, (i) **3**-CT-Acid-S**,** (j) **4**, (k) **4**-AcidCat, and (l) **4**-CT-Acid-S.

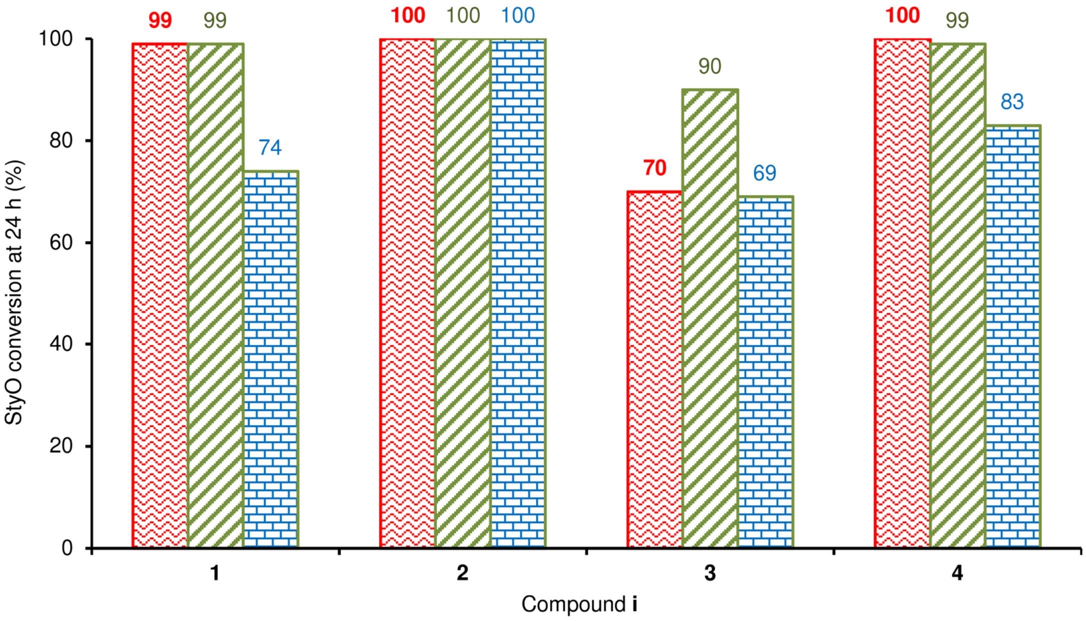

Fig. S7 Conversion of StyO with ethanol, at 24 h, 55 °C, in the presence of compounds **1**-**4** (red waves), the respective solids ***i***-CT-Acid-S (green diagonal lines), or using the solutions ***i***-CT-Acid-L (blue bricks) obtained from the contact tests for **1**-**4**.

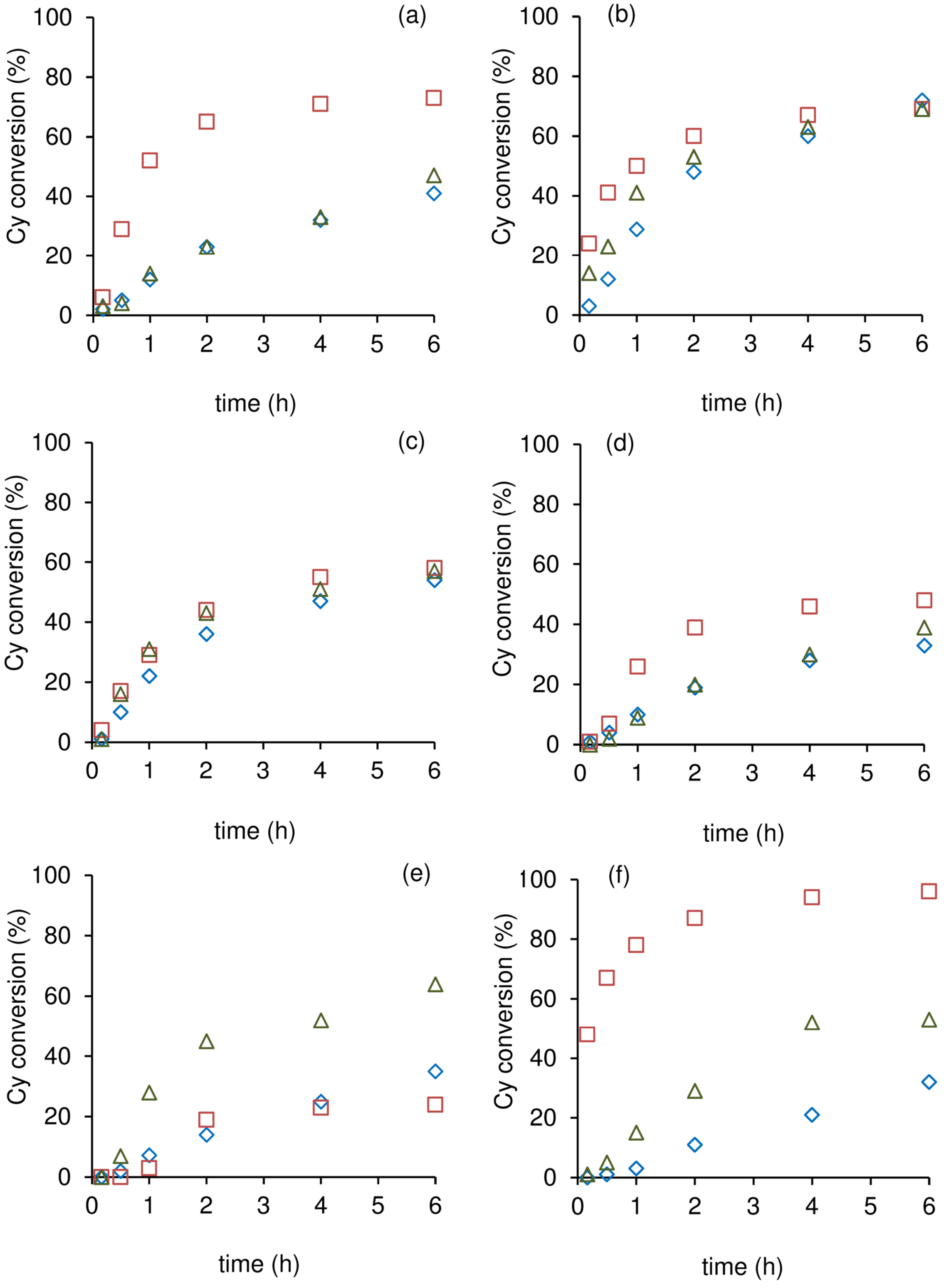

Fig. S8 Contact tests (CTs) carried out for (a) $[\mathrm{MoO_3}(2,2'\text{-bipy})]$ **1**, (b) $[\mathrm{Mo_2O_6}(2,2'\text{-bipy})]$ **2**, (c) $[\mathrm{Mo_3O_9}(2,2'\text{-bipy})_2]$ **3**, (d) $\{[\mathrm{MoO_3}(2,2'\text{-bipy})][\mathrm{MoO_3(H_2O)}]\}_n$ **4**, (e) $[\mathrm{MoO(O_2)_2}(2,2'\text{-bipy})]$ **5**, and (f) $\mathrm{MoO_3}$, at 55 °C. In each case kinetic profiles for Cy epoxidation are compared for reactions performed using the original catalyst (◊), the respective recovered solid ***i***-CT-TBHP-S (***i*** = **1**-**5** or $\mathrm{MoO_3}$) (△), or the solutions (***i***-CT-TBHP-L) of the CTs (□).

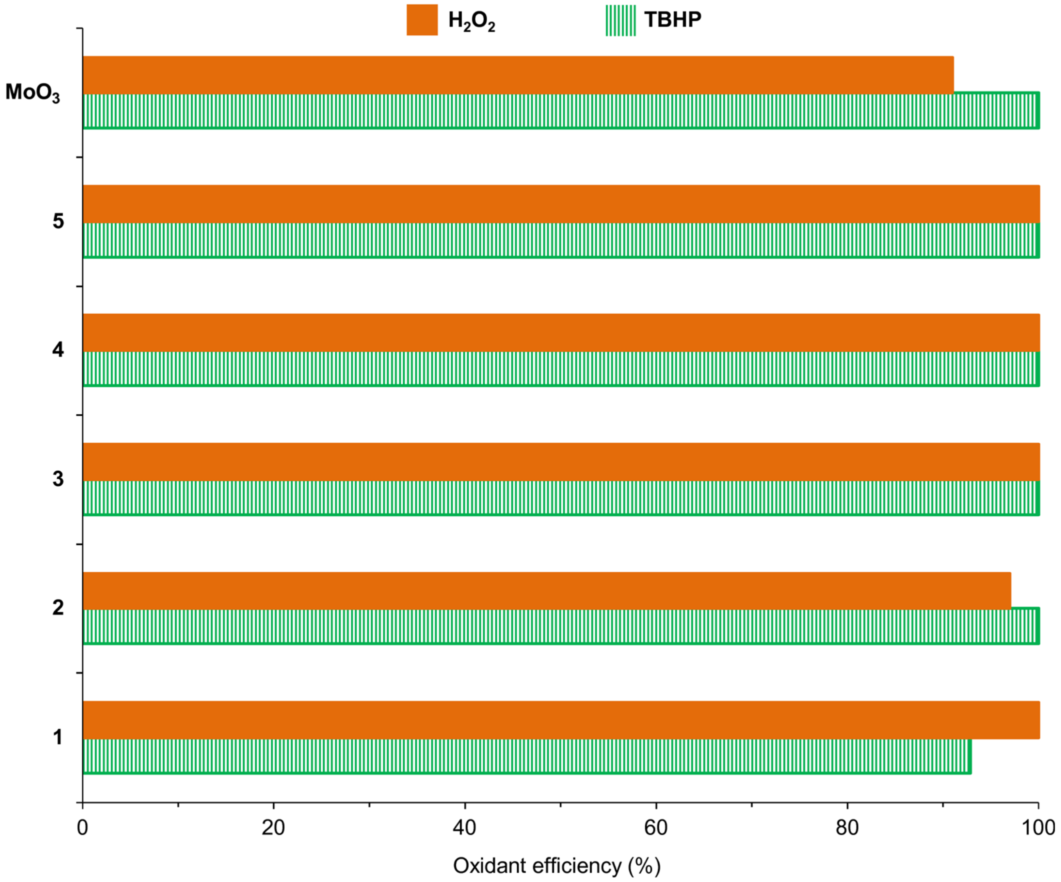

Fig. S9 Oxidant efficiency (determined for 24 h reaction) for the different catalysts, at 55 °C.

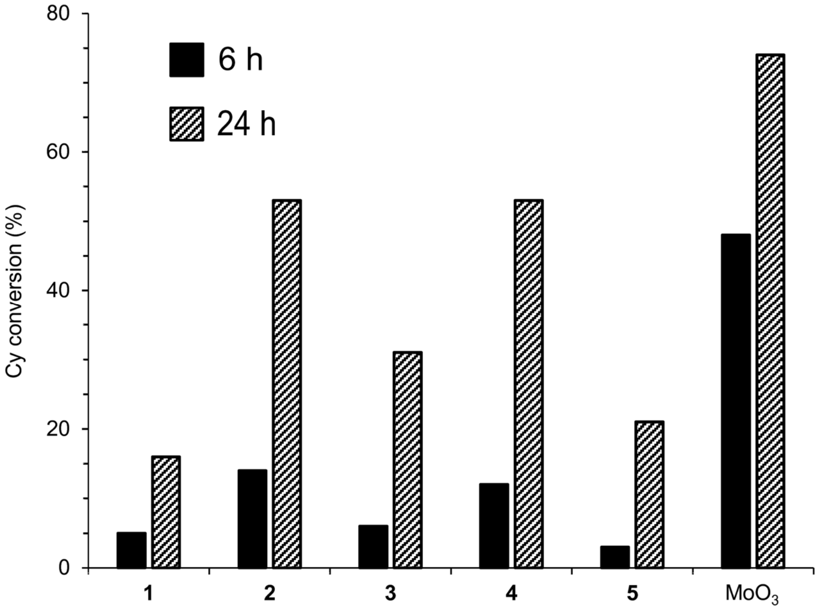

Fig. S10 Cy conversion using H_2O_2 as oxidant, in the presence of **1-5** or MoO_3, at 55 °C.

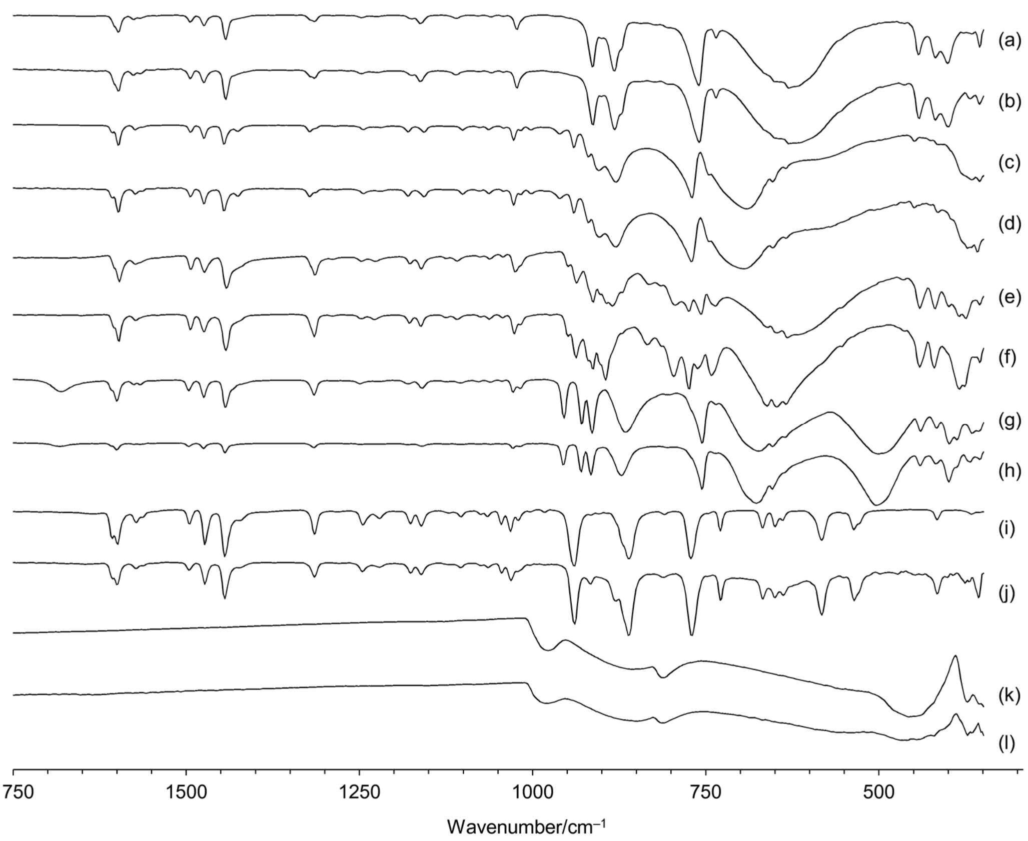

Fig. S11 ATR FT-IR spectra of (a) **1**, (b) **1**-Cat-TBHP, (c) **2,** (d) **2**-Cat-TBHP, (e) **3**, (f) **3**-Cat-TBHP, (g) **4**, (h) **4**-Cat-TBHP, (i) **5**, (j) **5**-Cat-TBHP, (k) MoO_3, and (l) MoO_3-Cat-TBHP.

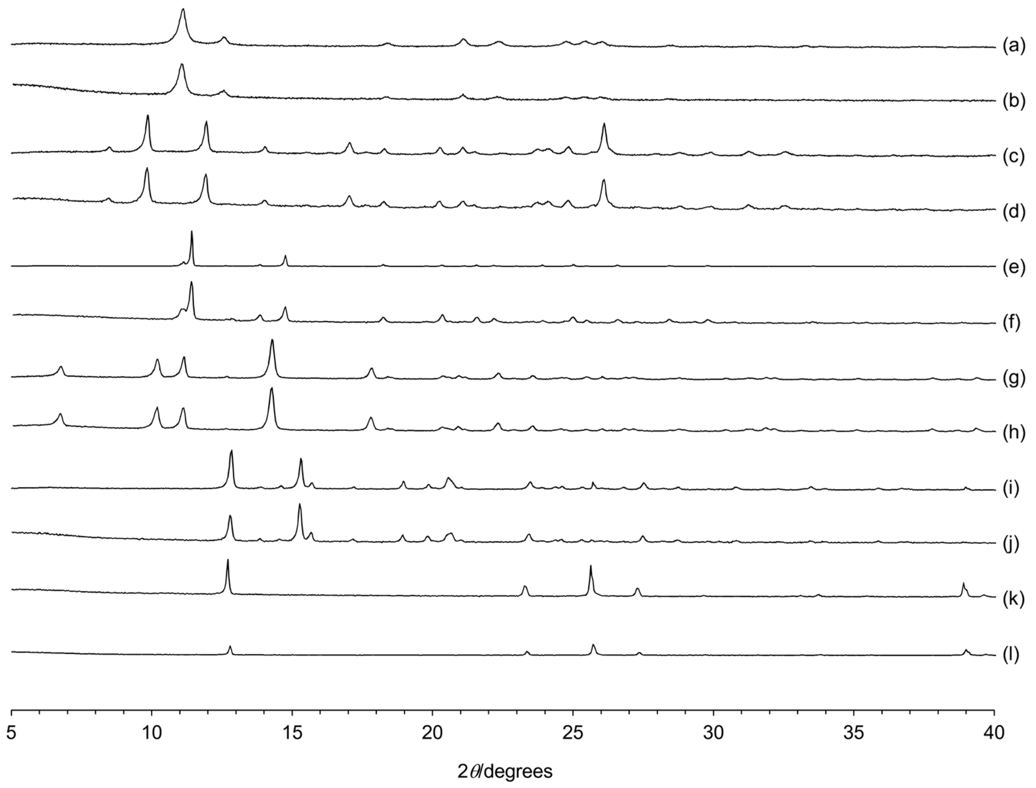

Fig. S12 PXRD patterns of (a) **1**, (b) **1**-Cat-TBHP, (c) **2,** (d) **2**-Cat-TBHP, (e) **3**, (f) **3**-Cat-TBHP, (g) **4**, (h) **4**-Cat-TBHP, (i) **5**, (j) **5**-Cat-TBHP, (k) MoO_3, and (l) MoO_3-Cat-TBHP.

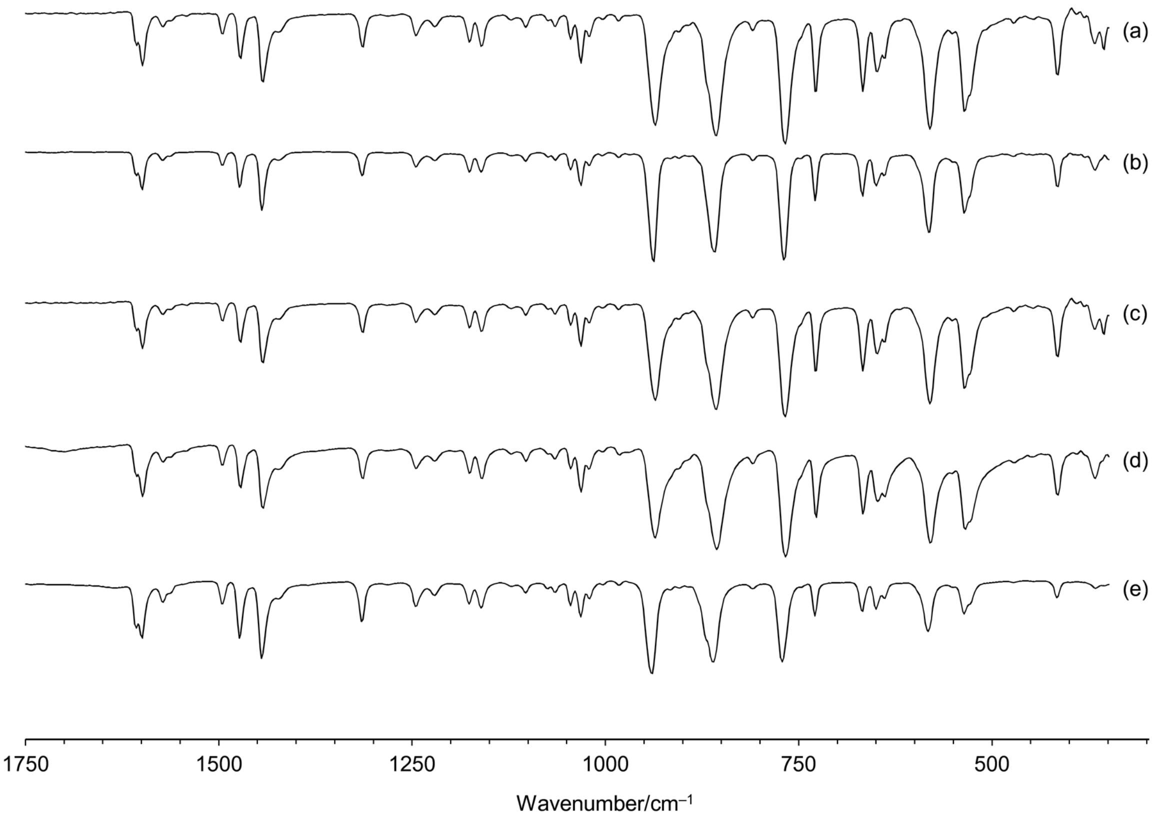

Fig. S13 ATR FT-IR spectra of (a) **1**-Cat-H_2O_2, (b) **2**-Cat-H_2O_2, (c) **3**-Cat-H_2O_2, (d) **4**-Cat-H_2O_2, and (e) **5**.

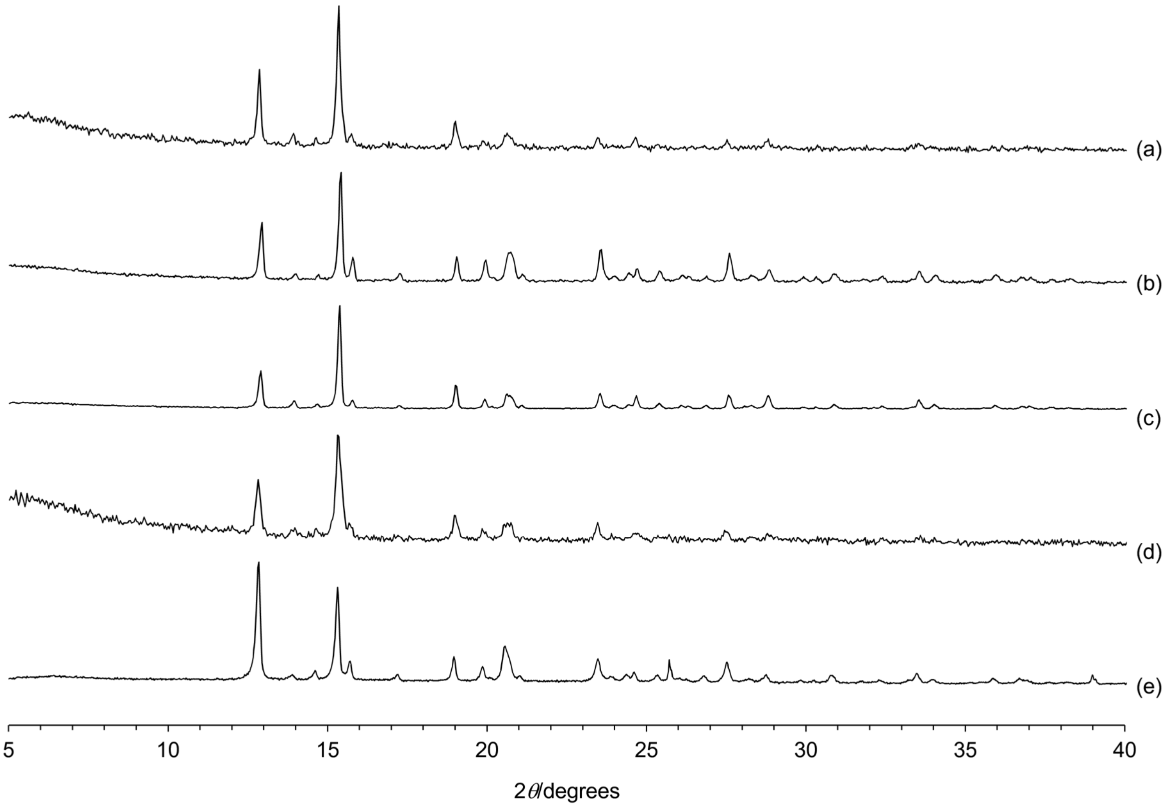

Fig. S14 PXRD patterns of (a) **1**-Cat-H_2O_2, (b) **2**-Cat-H_2O_2, (c) **3**-Cat-H_2O_2, (d) **4**-Cat-H_2O_2, and (e) **5**.

References

1 C. F. Macrae, I. J. Bruno, J. A. Chisholm, P. R. Edgington, P. McCabe, E. Pidcock, L. Rodriguez-Monge, R. Taylor, J. van de Streek and P. A. Wood, *J. Appl. Crystallogr.*, 2008, **41**, 466-470.

2 P. J. Zapf, R. C. Haushalter and J. Zubieta, *Chem. Mater.*, 1997, **9**, 2019-2024.

3 M. Abrantes, T. R. Amarante, M. M. Antunes, S. Gago, F. A. A. Paz, I. Margiolaki, A. E. Rodrigues, M. Pillinger, A. A. Valente and I. S. Gonçalves, *Inorg. Chem.*, 2010, **49**, 6865-6873.

4 E. O. Schlemper, G. N. Schrauzer and L. A. Hughes, *Polyhedron*, 1984, **3**, 377-380.

5 N. Anbu and A. Dhakshinamoorthy, *J. Ind. Eng. Chem.*, 2018, **58**, 9-17.

6 L. Zhang, C. Hu, W. Mei, J. Zhang, L. Cheng, N. Xue, W. Ding, J. Chen and W. Hou, *Appl. Surf. Sci.*, 2015, **357**, 1951-1957.